Agricultural and Forest Meteorology 291 (2020) 108036

Contents lists available at ScienceDirect

Agricultural and Forest Meteorology

journal homepage: www.elsevier.com/locate/agrformet

Climatic and anthropogenic influence on tree-ring growth in riparian lake forest ecosystems under contrasting disturbance regimes

Gianluigi Mazza*, Claudia Becagli, Roberta Proietti, Piermaria Corona

CREA Research Centre for Forestry and Wood, 52100 Arezzo, Italy

A R T I C L E   I N F O

Keywords:
Climate-growth relationships
Tree-rings analysis
Water level fluctuations
Riparian vegetation
Dendroecology
Drought

A B S T R A C T

In the Mediterranean region, the coupled effect of recent changes in climatic features and an increase in human-related water demand induced a progressive reduction in the water level of many lakes. Consequently, intense withdrawals for public supply can affect the health of lake ecosystems and increase trees' vulnerability to predicted drought intensification effects.

This study aimed to evaluate, through a dendroecological analysis of riparian trees, the strength of the climatic and hydrological signals retained in the tree-ring widths and to detect a critical water-level threshold affecting tree resilience and growth recovery. Our study area is located within the Regional Natural Park of Bracciano-Martignano in central Italy. In recent years, the lake water-level drop observed at Bracciano after intensive water withdrawals raised concerns about the ecological impacts on the ecosystem's vulnerability.

The main distinctive pattern in the climate-growth relations was the influence of previous years precipitation and drought conditions up to five years at Bracciano. At Martignano, where lake water withdrawals are absent, long-term climatic signals disappeared after two years. The intensive human water use at Bracciano Lake most likely induced trees to be more dependent on groundwater raising or soil water content stored from the previous rainy periods especially on an annual scale. On the other hand, tree-ring growth was strongly correlated with short-term water-level fluctuations (monthly – seasonal).

Tree-rings of riparian species appear to be a useful tool to detect critical water levels after the intensive water withdrawals and the increase in dry conditions occurred in the past few decades. Yearly values ranging from -108 to -139 cm may be considered as potential thresholds affecting riparian species. This finding may support lake water withdrawal regulation for riparian ecosystem protection and conservation under future drought intensification.

1. Introduction

Over the past few decades, several stressors, including human influence, have largely reduced the ecological resilience of many ecosystems through various local impacts that interact with global changes (Gunderson, 2000; IPCC, 2007), increasing their vulnerability. Lake ecosystems represent important sentinels of climate change, because they provide indicators of climate change either directly or indirectly through the influence of climate on the catchment (Adrian et al., 2009). The variations in seasonal and interannual precipitation, drought, and human-related water demand have significantly changed the water-level fluctuations, which are an essential component of the health of these ecosystems (Zohary and Ostrovsky, 2011; Gownaris et al., 2018).

In the Mediterranean region, during the past few decades many lakes have experienced a progressive drop in the water level both climate-driven and human-induced (Naselli-Flores and Barone, 2005; Papastergiadou et al., 2010). Undoubtedly, climate plays a crucial role in controlling the hydrology of lakes, determining both the inputs and outputs of water. However, water-level reduction can also be attributed to different human-induced factors, such as intensive agricultural activity and a rising need for water supply for domestic and industrial use (Crisman et al., 2005). Water-level reduction causes additional stresses to aquatic and surrounding terrestrial environments, and transitional areas such as riparian forests (Naiman et al., 2010), which are among the ecosystems most directly affected by water-level reduction, mainly because of a reduction in water availability (Merritt et al., 2010; Vesipa et al., 2017; You and Liu, 2018).

In identifying the direct influence of water availability on trees growth and stress, annual growth rings are one of the best proxy because they can reflect hydrologic signatures such as variation in water

* Corresponding author.
E-mail address: gianluigi.mazza@crea.gov.it (G. Mazza).

https://doi.org/10.1016/j.agrformet.2020.108036
Received 8 March 2020; Received in revised form 7 May 2020; Accepted 9 May 2020
0168-1923/

Table 1
Main characteristics of the tree species sampled in the Bracciano e Martignano lakes. N: number of trees, BA: total basal area, DBH: mean diameter at breast height; mean age ± standard deviation.

Species	Bracciano				Martignano			
	N	BA (m^2)	DBH (cm)	Age (year)	N	BA (m^2)	DBH (cm)	Age (year)
Alnus g.	96	4.09	23.3	27 ± 8	16	1.00	28.2	17 ± 3
Populus spp	12	0.60	35.6	24 ± 5	19	1.19	28.2	18 ± 4
Salix spp.	15	1.21	32.1	21 ± 4	36	4.33	39.2	19 ± 4
Tot	*123*	*5.90*	*30.3*	*24 ± 6*	*71*	*6.52*	*31.9*	*18 ± 4*

availability (Stockton and Fritts, 1973; Fritts, 1976; Amlin and Rood, 2003; Rains et al., 2004; Snyder and Williams, 2007).

Riparian tree species are among the least investigated in dendrochronological studies (Grissino-Mayer, 1993; Netsvetov et al., 2019). Synchronization of tree-ring series of riparian species is difficult due to the high frequency of intra-annual density fluctuations together with the relatively short life span of many tree species found in these habitats (Seiwa et al., 2005). Despite riparian forest's conditions issues, in recent decades, tree-ring growth of riparian vegetation has been successfully used as an indicator of geomorphologic processes, model catchment hydrology, water-level reconstruction and modelling, and hydrological changes in wetland forests (Begin, 2001; Willms et al., 2006; Dufour and Piégay, 2008; Wiles et al., 2009; Rodrìguez-Gonzàlez et al., 2014; van der Maaten et al., 2015; Gomes Marques et al., 2018; Netsvetov et al., 2019).

The present study area is in central Italy within the Regional Natural Park of Bracciano-Martignano. The two lakes are influenced by the same climatic conditions but are characterised by contrasting disturbance regimes. Bracciano Lake experiences a greater water demand for urban and tourist activities than Martignano, where the anthropogenic impact is negligible. Bracciano Lake has been utilised as a potable water reservoir for the Vatican and the city of Rome since Roman times. In recent years, water-level decline was observed at the Bracciano Lake after intensive water withdrawals raised concerns about the ecological impacts on the ecosystem's vulnerability. Much attention has been focused on the effects of water withdrawal on the hydrologic system, but recent studies have also highlighted the increase in drought conditions as an additional important hydrological stressor (Taviani and Henriksen, 2015). Consequently, the coupled effects of changing climatic conditions and anthropogenic impacts can increase the vulnerability of these ecosystems, resulting in greater losses of ecological functions and services. In this context, the aims of this study were: i) to evaluate the strength of the climatic and hydrological signals in the main tree species growing along the shorelines of the two lakes, and ii) to detect a critical water-level threshold affecting tree resilience and growth recovery to support a more suitable lake water withdrawal.

2. Materials and Methods

2.1. Study sites and tree characteristics

Bracciano and Martignano Lakes are located 30 km north of Rome within the Regional Natural Park of Bracciano-Martignano (Special Protection Area – SPA, IT6030085). It was established in 1999 and inludes both natural areas and cultural sites that extend into the area of the Sabatini Mountains. The two lakes are at a distance of 2.5 km, and Martignano Lake is located at an elevation of about 50 m a.s.l. higher than Bracciano. Contrary to Martignano, Bracciano Lake is surrounded by small municipalities and infrastructures for touristic activities.

The soils belong to two types – Cambic Phaeozems (loamic) and Eutric Regosol (loamic) (IUSS Working Group WRB., 2015 – and are characterised by a sandy loam texture, a moderately acidic or neutral pH without carbonates and good or moderately good drainage (Napoli et al., 2019).

The most important water inflow is from precipitation directly on the lake and the most important outflows from the lake are evaporation from the surface and, for Bracciano Lake, withdrawals for supply. Although precipitation is the dominant source of water, at Bracciano it was found that the groundwater inflow to the lake can balance declining net precipitation trends and fluctuations in lake water levels, reducing lake level declines mainly during short periods of dry conditions (Taviani and Henriksen, 2015).

Based on direct soil coring at the beginning of December, in the first 10–15 m from the shoreline both at Bracciano and Martignano, groundwater was found at a depth of about 70–130 cm. During the driest summer period, this depth is lowered by about 20–50 cm depending on the water-level decrease.

The riparian woody vegetation covers an area of about 60 ha and is mainly scattered along the shorelines. It is mainly composed of black alder (*Alnus glutinosa* L. Gaertn.) formations, single trees or small groups of black poplar (*Populus nigra* L.) and white poplar (*Populus alba* L.), hydrophilic bushes with white and purple willow (*Salix alba* L. and *Salix purpurea* L.), and *Cytisus scoparius, Rubus* sp. and *Crataegus monogyna*. Upland contiguous forests are dominated by Turkey oak (*Quercus cerris* L.) and holm oak (*Quercus ilex* L.).

At Bracciano, the main species sampled was *Alnus glutinosa* with 78% of the total sampled trees, while at Martignano the main species were *Salix* spp. (51%). In both cases, the main species were diffuse porous deciduous broadleaves. The main dendrometric characteristics of the trees sampled are shown in Table 1.

2.2. Climatic characterisation

The climate data were recorded at the Bracciano meteorological station (284 m a.s.l) and cover the period 1950–2018. Standardised Precipitation-Evapotranspiration Index (SPEI) was calculated through Potential Evapotranspiration (PET) according to the Thornthwaite equation as implemented in the R package SPEI (Vicente-Serrano et al., 2010) using mean temperature values from the nearby Bracciano meteorological station data. SPEI is a multi-scalar drought index (Vicente-Serrano et al., 2010), computed to identify drought severity in the study area. SPEI values are based on the normalisation of the climatic water balance as the difference between cumulative precipitation and the PET for a given period at monthly intervals and ranges from −3 to 3. The use of SPEI is relevant to the quantification of the effects of droughts on tree growth because of its ability to capture the main impact of increased temperature on water demand (Vicente-Serrano et al., 2013). Monthly water-level records (WL, cm) were available only for Bracciano Lake (from 1921 to 2018) and they were provided by the Regional Natural Park.

The climate is typical Mediterranean with a mean annual rainfall of 931 mm concentrated mainly in autumn and winter and a dry summer in which July and August are the driest months with 23.8 and 23.1 mm of rainfall, respectively (Fig. 1). The mean annual temperature is 16.9°C, the thermotype is meso-Mediterranean and the ombrotype is sub-humid/humid lower (Blasi, 1994).

2.3. Tree sampling and dendrochronological analysis

Dominant straight trees without any injuries to the crown and stem

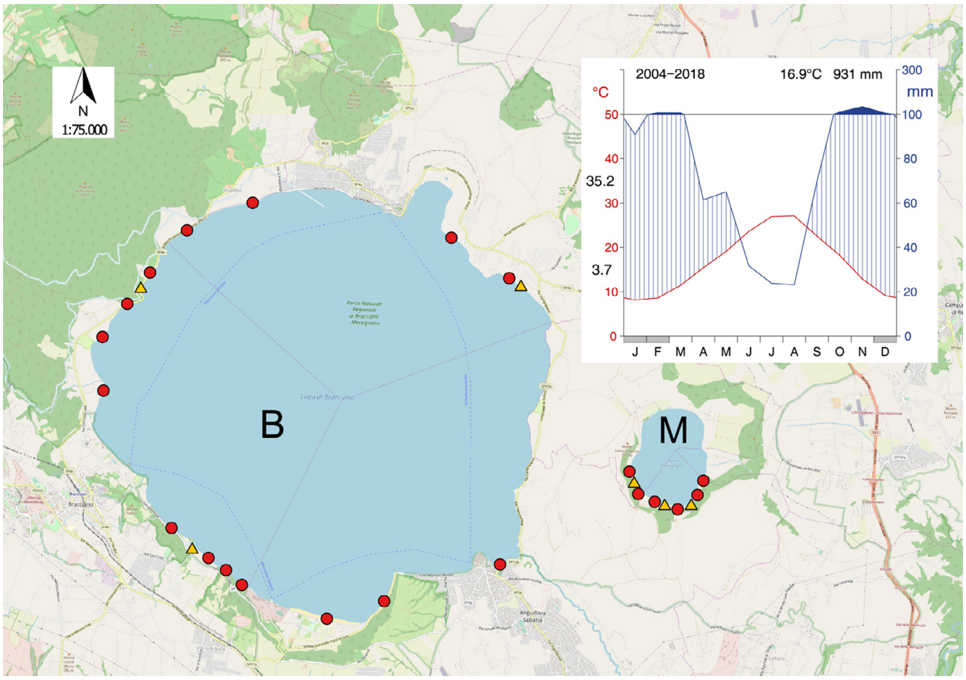

Figure 1. Location of riparian vegetation (circles) sampled along the shoreline of Bracciano (B) and Martignano (M) Lakes and Walter & Lieth (ombrothermic) climatic diagram of the study area. Average annual temperature and the total annual rainfall (top). Mean maximum temperature of the warmest month and mean minimum temperature of the coldest month (beside the left y-axis). The dotted area indicates seasonal water deficit. Triangles indicate soil coring for groundwater depth determination.

were selected along the lake's shorelines (Fig. 1). In multi-stemmed trees, only the largest stem with the dominant crown was sampled. The sampled trees were located on the floodplain surface elevation within the first 10–15 m from the shoreline.

Two cores per tree were extracted with a 5-mm diameter increment borer at breast height on the cross-sides of the trunk. Cores from a total of 194 trees were collected (123 at Bracciano and 71 at Martignano).

The increment cores were mounted on wooden supports, air-dried and then smoothed with the slide microtome WSL-Core-microtome (Gärtner and Nievergelt, 2010). Transverse micro-sections with 15–20 µm thickness and 10–20 cm length was cut from the entire increment cores using the above-mentioned slide microtome. Micro sectioning easily allows detecting the ring structure of many deciduous species, which is hardly visible macroscopically on sanded or even on cut core surfaces (Gärtner et al., 2015). The possibility of taking micro-sections from entire tree cores in combination with a short processing time could overcome this difficulty (Gärtner et al., 2015). Since glass slides of the required dimensions are not available at common laboratory equipment companies, a common high-quality glass was used. It is available in every common glassware store and is easy to cut to the required dimension, resulting in a quite cheap solution. The long micro-sections were stained and prepared according to the standard laboratory protocol (Werf van der et al., 2007; Gärtner et al., 2015).

Annual tree-ring widths (TRW) were measured from bark to pith with a 0.01-mm precision by a computer-linked measuring table (LINTAB™ 6, Rinntech, Germany) under a stereo microscope (Leica S9i, magnification range: 6.1X – 55X) and a software package (Time Series Analysis and Presentation, TSAP, Frank Rinn, Heidelberg, Germany). For this aim, the glass slides with the micro-sections were placed under the stereo microscope on a special support raised from the measuring table and were analyzed in transmitted light by inserting optical fibers from below (Fig. S1). When a particular TRW measurement was uncertain due to the tree ring structure (narrow rings and/or false rings), the slides were additionally checked under the transmitted light microscope ZEISS AXIO Lab. A1 (magnification range: 50X – 400X). Images were acquired through the ZEISS AxioVision 4.8.2 SP1 software. If the dating difficulty remained, these cores were discarded.

Each ring-width series was first visually checked and then statistically verified for cross-dating and measurement errors using TSAP and "dplR" developed for the R software environment (Bunn, 2010). Trees with a Cross Date Index (CDI) below 10 (Rinn, 2012) and a correlation with the master chronology below 0.4 were discarded from further analysis. CDI is a powerful parameter for the matching of chronologies, based on the combination of two parameters: i) t-values and ii) 'Gleichlaeufigkeit' (GL). The cambial age of cores containing the pith was determined by counting the calendar years assigned to the tree rings from bark to pith.

To remove age-related growth trends and competition effects, a one-step detrending was applied to each mean tree-ring series using the package dplR (Bunn 2008). Due to the short time-span of chronologies, the mean function was fitted to each ring-width series and detrended the original series by calculating ratios. The index values were then prewhitened using an autoregressive model selected on the basis of the minimum Akaike information criterion and combined across all series using a bi-weight robust estimation of the mean (Cook & Kairiukstis, 1990). The detrending method applied allows to still preserve the autocorrelation from tree-ring chronologies, retaining both low and high-frequency climatic signals. It allows identifying any possible effects on tree growth of previous years' climatic or hydrological variables, which are strongly autocorrelated. The mean correlation between trees (r.bt) was computed to assess the synchronization in the annual growth patterns among sampled trees and the common signal strength indicated by the mean growth chronologies. The chronology reliability was tested using the Expressed Population Signal (EPS) (Wigley et al., 1984). Only those series with a high common signal (EPS $\geq$ 0.85) were included in the analysis.

We categorized species into a single functional group based on their common xylem architecture (diffuse porous) and phreatophitic behaviour (Allen et al.,1999; Cox et al., 2005; Singer et al., 2013; Elliot et al., 2015). After testing the similarity in trends and synchronization of the mean chronologies among the three riparian species sampled, we found highly significant correlations mainly at the site level (Table 2 and Fig. S2). This coherent pattern suggests that a common factor similarly affected the species (Gebrekirstos et al., 2008), producing a high degree of common variation shared by the riparian tree species at each site. Therefore, to emphasize mutual characteristics of species chronologies discriminating against the two sites, a total of 98 trees and 131 cores were used to compute the mean site chronologies (Fig. 2 and Table 3), combining *Alnus glutinosa, Populus spp*. and *Salix spp*. with the following species frequency: 64, 14 and 22 % at

Table 2
Correlation coefficients and Gleichläufigkeit statistic (percentage of common signs of year-to-year growth change between two series, Glk – Buras and Wilmking, 2015) among the mean chronologies of the main three riparian species at Bracciano (B) and Maritgnano (M). Bold values indicate coefficients at the site level.

Spearman	Populus B	Salix B	Alnus M	Populus M	Salix M
Alnus B	**0.77*****	**0.87*****	0.55*	0.38	0.41
Populus B		**0.78*****	0.46*	0.52*	0.45*
Salix B			0.58*	0.32	0.38
Alnus M				**0.86*****	**0.87*****
Populus M					**0.87*****
Glk	Bracciano 0.71			Martignano 0.75	

GlK is a measure of the agreement between the interval trends of two curves.

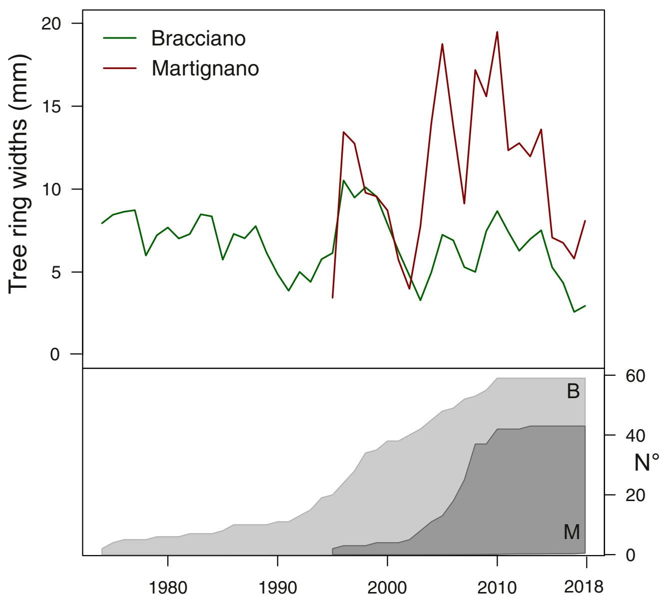

Figure 2. Chronologies for raw tree-ring widths (TRW). The shaded areas indicate the number of trees sampled.

Table 3
Main dendrochronological statistics of the study sites. Mean ring width (MRW), Glk, CDI - Cross Date Index, mean sensitivity (MS) and first-order serial autocorrelation (AC1), computed for the raw tree ring series; mean inter-serial correlation (r.bt) and expressed population signal (EPS), computed for the standardized tree-ring series. FRs: false rings.

	Bracciano	Martignano
Time span	1974-2018	1995-2018
(N° years)	(45)	(24)
N° cores/N° trees	76/58	55/40
MRW ± SD (mm)	6.9 ± 3.8	12.1 ± 6.7
Glk	0.58	0.58
CDI	14	13
SM	0.419	0.421
AC1	0.40	0.38
r.bt	0.45	0.44
EPS	0.95	0.95
Trees with FRs (%)	71.2	26.2
Rings with FRs (%)	9.4	2.9

Bracciano, 18, 40 and 42 % at Martigano, respectively.

The mean tree-ring width of the Martignano chronology was almost twice that of Bracciano (12.1 and 6.9 mm, respectively) and mean sensitivity (MS) was about 0.42 at both sites. Synchronisation between mean site chronologies was significant both for the raw and standardised tree-ring width series as well as for the basal area increments, especially in the last decade (Fig. 3). Indeed, the Spearman correlation coefficient (*rho*) is passed from 0.48 ($P < .05$) in the entire common period to 0.91 ($P < .001$) in the last ten years.

Most of the detected false rings (FRs) were in the cores of Bracciano in a percentage of trees 2.7 times greater than Martignano (Table 3), and their formation did not appear to be species-specific.

2.4. Climate-growth relationships

Considering the rapid juvenile growth of riparian tree species, which can reach 1.3 m by their second year (Harrington and Curtis, 1986), climate-growth correlations were tested by removing the first five years with the aim to reduce the influence of non-climatic factors on tree growth variability during the establishment phase typical of the first years of growth, when the climatic signal is not well retained in tree-ring widths (e.g., due to strong competition with shrubby understory vegetation). For black alder, for example, this phase was considered to be up to age 7–10 and, based on most of the height growth curve models, it was characterised by very high growth rates (Thibaut et al., 2004; Claessens et al., 2010). The influence of climate on tree-ring growth at 1-month and seasonal timescale was investigated over a common period using a correlation function (CF) analysis (Fritts 1976) based on Pearson's correlation coefficient. We used 15 monthly climatic variables (for precipitation - P and SPEI) sequenced from September of the year prior to growth (t-1, uppercase acronyms) to November of the current year of growth (t, lowercase acronyms), assuming that the cambial activity continues during autumn because of the favourable growth conditions of the riparian environment.

Seasonal climate-growth correlations were checked at 3-months timescale from August (t-1) to November (t) using 14 seasonal periods of three months (e.g. October-November-December, OND; November-December-January, NDj; December-January-February, Djf, etc.) and shifted every time of one month. To increase the cumulative effect of seasonal climatic variables, 11 periods of six months from ASONDj to jasond were analysed.

Pearson's correlation coefficients were tested for significance using the 95 % percentile range method after a bootstrap process, adopting 1000 replications with the "treeclim" package in R programme (Zang and Biondi, 2015).

In identifying any possible effects of previous years' precipitation and SPEI, on tree growth, we tested over the common period antecedent climatic variables up to 5 years prior to the current year of tree-ring formation, calculated as the sum (for precipitation) or average (for SPEI and water level) of the *i*-esimo previous year: $t + t_{-i}$, where t is the value of the current year and i ranges from 1 to 5. Climate–growth relationships at annual scale were investigated using the Pearson's correlations after testing for normal distribution with the Kolmogorov-Smirnov and Shapiro-Wilk tests. Since we were not concerned with the simultaneous testing of all correlations, no Bonferroni correction was applied to significance levels (Perneger, 1998).

Besides, to evaluate tree-ring growth responses to severe drought events (monthly, seasonal and annual precipitation and SPEI values below the 5th percentile) the Superposed epoch analysis (SEA) as implemented in the R package "dplR" was used. This function calculates the significance of the departure from the mean for a given set of key event years and lagged years. SEA computation is based on scaled RWI values, and 95%-confidence intervals are computed for the scaled values for each year in the superposed epoch.

2.5. Growth responses to hydrological factors

As for precipitation and SPEI, the influence of water level (WL) on tree-ring growth was investigated using Pearson's correlations, testing the same range of variables at monthly, seasonal and annual scale.

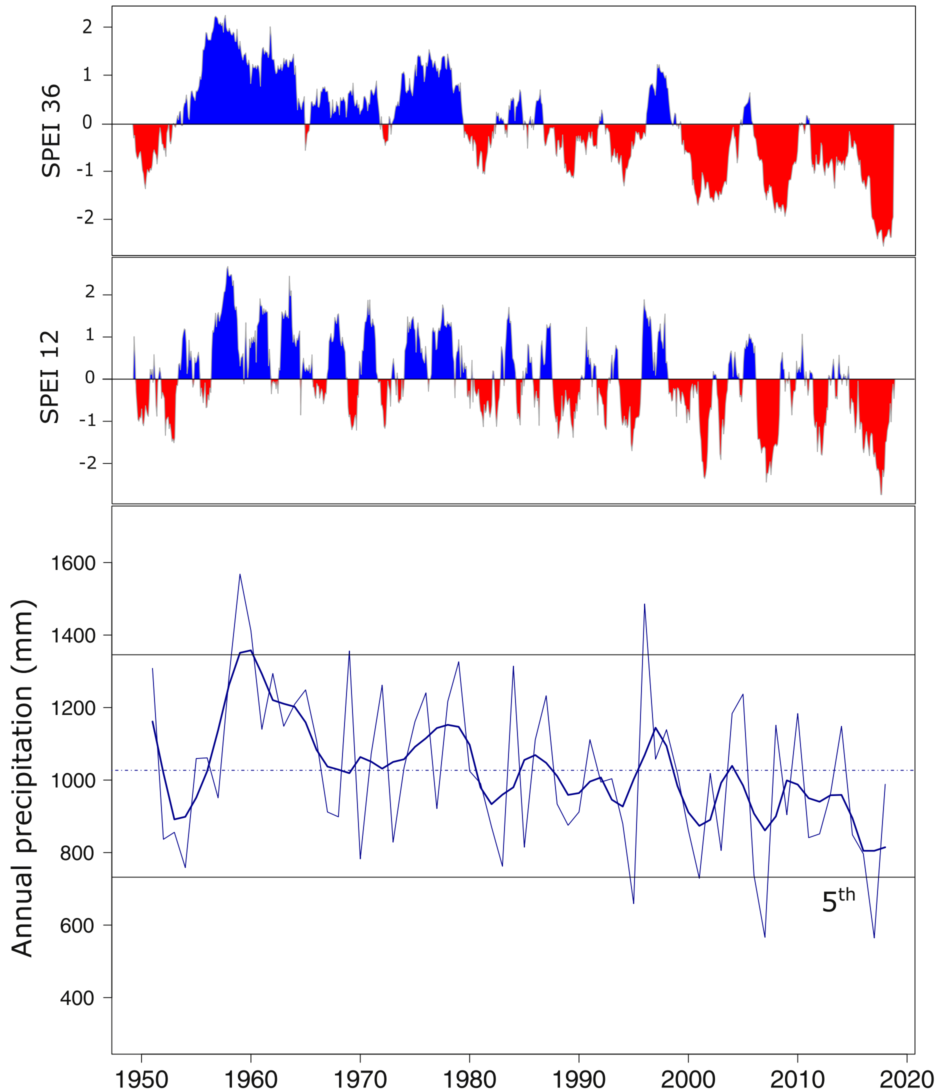

Figure 3. Annual precipitation with 5th percentile-based thresholds and SPEI index at the timescale of 12 and 36 months.

Moreover, after identifying the lowest water levels those values below the 10th and 5th percentile, we determined pointer years as those years in which most series showed a significant TRW reduction using the relative growth change method (Schweingruber et al., 1990). Thus, the lowest water levels were defined as critical when there was a significant impact on tree ring growth. This way, a negative pointer year was considered when at least 75% of the TRW series displayed an event year with a TRW decrease of at least 40% relative to the average TRW in the 3 preceding years.

In evaluating the effect of critical water levels (CWL) on tree growth dynamics, we calculated resistance (Rt), resilience (Rs) and recovery (Rc) indices linked to components of growth stability, as follows (from Lloret et al., 2011; Marqués et al., 2016; Gomes Marques et al., 2018; modified):

- Resistance (Rt): $Rt = CWL_0/CWL_{pre}$
- Resilience (Rs): $Rs = CWL_{post}/CWL_{pre}$
- Recovery (Rc): $Rc = CWL_{post}/CWL_0$

where CWL_0 is the tree-ring growth corresponding to the year of critical water level, CWL_{pre} and CWL_{post} are the tree-ring growth in the years before and after the critical water level, included between two successive critical years. The R package "PointRes" was used to compute the pointer years and resistance, resilience and recovery indices (van der Maaten-Theunissen et al., 2015).

2.6. Statistical methods

2.6.1. Trends and spectral analysis

To assess the presence of temporal trends in the climatic time series, we applied the Mann-Kendall non-parametric test (τ) (Brunetti et al. 2006; Hamed 2008).

To explore common patterns between hydroclimatic variables, we expressed the characteristics of our time series in the frequency domain. The spectral methods are useful to assess the main features of a climate time series, which are typical random variables of stochastic processes available in discrete time, and not in continuous time (Ghil et al., 2002). In this case, the multi-taper spectral analysis (MTM) was performed. If there is a consistent periodic climate (or environmental) signal with frequency f (from zero up to the Nyqvist frequency 0.5 $year^{-1}$) represented in the data, this signal should appear as a spectral peak accompanied by an F-test value above the critical level (here, 95% and 99% significance levels).

Wavelet-based spectral analysis was applied both to the water level and climate variables time series to perform a multiscale wavelet correlation analysis. Wavelets are derived from a one-dimensional multiresolution analysis performing an additive decomposition of the original time series from 2 to 2^4 years (wavelet detail D1, D2, D3 and D4)

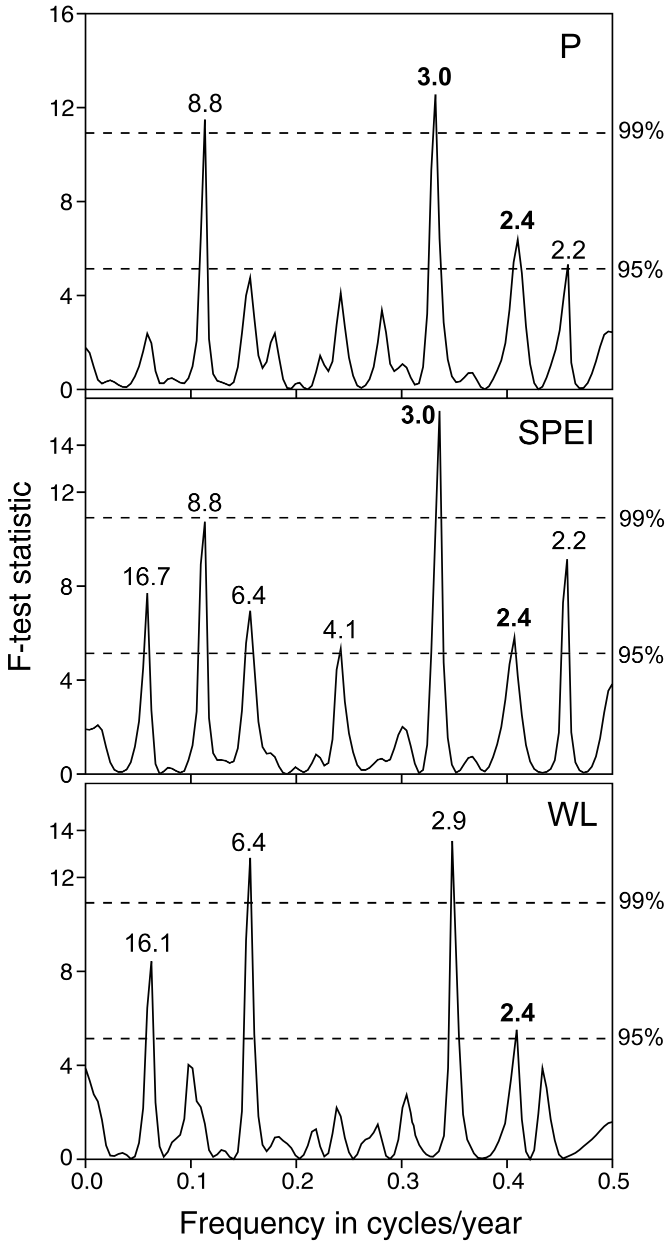

Figure 4. Multi-Taper Spectrum (MTM) for yearly precipitation, SPEI and water levels (WL). Horizontal dotted lines indicate 95% and 99% significance levels. Numbers indicate significant and common (in bold type) spectral peaks.

based on the "Maximal Overlap Discrete Wavelet Transform - MODWT" method (Torrence and Compo, 1998; Percival and Walden, 2000; Bunn, 2008). The Bonferroni method was used to correct the significance levels for multiple comparisons of paired hydroclimatic time series. The multiscale wavelet correlations helped us to further evaluate the similarity between water-level fluctuations and climate variables at both high and low frequencies.

2.6.2. Partial least squares regression (PLSR)

For the period 2007–2016, tree-ring growth was also correlated with the main hydrological variables of the lake water balance such as lake evaporation (E), water reservoir (WR) and water withdrawal (WW) taken from Boni et al. (2017). As reported in this article, lake evaporation (E) has been estimated as a function of the average monthly temperature and Thornthwaite monthly solar index. WR has been estimated as: WR = P - E - ETR, where ETR is the evapotranspiration. WW refers to those from Bracciano Lake carried out by the water management agency of Rome (ACEA).

Over the same period, we performed the partial least squares regression (PLSR, using R package "plsdepot") to evaluate how the most significant climatic drivers based on the previous correlation analysis and how the hydrological factors (the independent variables) influenced tree-ring growth (the dependent variable or response variable; Appendix S1). To our knowledge, this was the first attempt to explain the tree-ring growth variability of riparian species by a rather exhaustive set of hydroclimatic variables in a lake basin.

PLSR is a non-parametric method; no specific distribution is required and there is no assumption about the independence of observations (Lowry and Gaskin, 2014; Hair et al., 2017). PLSR is especially useful when 1) the number of predictor variables is similar to or higher than the number of observations (i.e. overfitting) and/or 2) predictors are highly inter-correlated (i.e. there is strong collinearity), which is a constraint for other regression techniques (Carrascal et al., 2009).

PLSR was tested using standardised tree-ring widths (RWI), and two components were always retained. Model strength was assessed by the sum of the R^2 of the two significant components and the proportion of variance in the dependent variable that can be predicted by the model (goodness of prediction, Q^2). A component is considered significant when Q^2 exceeds a critical value of $Q^2_{limit} = 0.097$ (Tenenhaus, 1998). To estimate the prediction error, we calculated the root mean square error of cross-validation (RMSECV) and the residual predictive deviation (RPD), defined as the ratio of the standard deviation of the response variable to the RMSECV. RPD superior to 3 is considered acceptable and RPD superior to 5 is considered excellent (Fearn, 2002). To facilitate the interpretation of the PLSR models and identify which predictor variables are most useful for predicting the response variable, we used the variable influence on projection (VIP) statistic, an index that pools the information over all predictors and PLSR dimensions (all retained components), resulting in one value for every predictor. Influential variables were assumed to have VIP > 1 (Paulo et al., 2015).

All the data analysis was performed in the R software environment (R Development Core Team, 2019. http://cran.r-project.org/).

3. Results

3.1. Hydroclimatic signals and trends

Total annual precipitation have decreased since 1960, showing a significant downward trend to date (τ = -0.31 with $p < .001$). During the last two decades (2000–2018), total annual precipitation decreased by 9 and 15% when compared to the previous 20 years (1980–1999) and the previous half-century (1950–1999), respectively. Moreover, since the 1990s, a significant increase in drought conditions was found (Fig. 3). Indeed, in the period of 2000–2018, the SPEI index at the timescale of 12 months was -0.26, while in the previous 20 years (1980–1999) it was close to zero and in the previous period (1950–1980) it was positive (0.19).

Water levels of Bracciano Lake at a yearly scale showed significant downward trends since the beginning of the data collection (1921), and especially since 1960 (τ = -0.35 and -0.49 with $p < .001$, respectively). During the last two decades (2000–2018), it reached the minimum level of about 100 cm below the hydrometric zero (the reference altitude above sea level), a decrease of 34 and 56% when compared with the averages of the previous twenty years (1980–1999, -65 cm) and the period from 1950 to 1980 (-43 cm).

Multi-taper spectral analysis of yearly precipitation, SPEI, and WL for the period of 1950–2018 revealed common significant peaks within the high-frequency domain (at 2.4 and around 3.0 years, Fig. 4). Moreover, the multi-taper spectral estimates of yearly SPEI and WL produced a similar cyclic pattern with two other common peaks at 6.4 years and at low frequencies around 16–17 years (Fig. 4).

Yearly WL were significantly correlated with both precipitation and

Table 4
Correlation coefficients at yearly scale between precipitation (P), standardised precipitation-evapotranspiration index (SPEI) and summer water-levels (WL) of Bracciano lake, considering the cumulative effect of past climatic conditions up to five previous years ($t + t_{-5}$). Correlation coefficients were also provided considering band-pass time series of the previous three variables from 2 to 2^4 years decomposed via multi-resolution analysis (wavelet detail D_1, D_2, D_3 and D_4).

ρ (Spearman)	Year	Yearly P	SPEI		Wavelets P	SPEI
	t	0.40**	0.53**	D_1	0.22	0.34
Bracciano	$t + t_{-1}$	0.66***	0.74***	D_2	0.24	0.39**
(1951-2018)	$t + t_{-2}$	0.75***	0.82***	D_3	0.38**	0.58***
	$t + t_{-3}$	0.74***	0.78***	D_4	0.64***	0.66***
	$t + t_{-4}$	0.71***	0.75***			
	$t + t_{-5}$	0.71***	0.75***			

Coefficients are significant at: * $p < 0.05$;
** : $p < 0.01$;
*** : $p < 0.001$.

SPEI, especially considering their effect accumulated over consecutive years (Table 4).

The wavelet analysis also confirmed the significance of the correlations between WL and precipitation and SPEI in the frequency domain, with the correlation coefficients increasing from high- to low-frequency signals (Table 4).

The influence of precipitation and SPEI was also significant on the seasonal scale. The highest correlation coefficients were found between summer WL (June, July and August) and winter (previous December, current January and February) precipitation and SPEI (ρ = 0.57 and 0.59 with $p < .001$, respectively).

3.2. Climate-growth relationships

Overall, at the Bracciano site we found a higher climate sensitivity than at Martignano. The main distinctive pattern resulting from the climate-growth analysis was the contrasting influence of long-term climatic variables, especially on an annual scale. Indeed, we found a greater influence of six months and especially multiple-years variables at Bracciano than at Martignano, both for precipitation and SPEI (Figs. 5 and 6).

For precipitation, at the monthly scale, the Bracciano chronology was more sensitive to April and June of the current year, while the Martignano chronology to November and December of the previous year, and November of the current year. At the seasonal scale, the positive influence of previous precipitation at Bracciano started early in the autumn (SON). During the current year, tree-ring growth at Bracciano was slightly influenced by summer precipitation, while Martignano chronology was strongly correlated with that of the autumn season. Considering the accumulated period of 6 months, the influence of previous precipitation at the Bracciano site was more significant than at Martignano (Fig. 5).

On an annual scale, at Martignano the highest correlation coefficients were found with the precipitation of the current year (t) and precipitation accumulated from the previous year ($t + t_{-1}$) and remained slightly significant up to 3 years ($t + t_{-3}$). At Bracciano, the influence of previous precipitation remained highly significant up to 5 years ($t + t_{-5}$; Fig. 5).

Regarding SPEI, the correlation pattern between the two sites was similar to that of precipitation, especially at the monthly scale (Fig. 6). At the seasonal scale, the main difference was again the significant influence of summer SPEI at Bracciano. Moreover, the effect of previous autumn was significant also at Martignano. On an annual scale, SPEI highlighted similar results as precipitation, showing significant correlations up to five years at Bracciano ($t + t_{-5}$), while at Martignano the significant effect of previous drought years disappeared after two years ($t + t_{-2}$; Fig. 6).

The superposed epoch analysis (SEA) confirmed a greater significant relationship between the key events at seasonal and annual scale and tree-ring growth at Bracciano than at Martignano, both for precipitation and SPEI (Fig. 7). The greater influence of long-term climatic variables on tree-ring growth at Bracciano, as resulting from the climate-growth analysis, again appeared as the main distinctive pattern between the two sites. Indeed, after testing all the significant climatic variables correlated with tree-ring growth, the effect of seasonal and especially annual key events remained significant over a greater number of following years at Bracciano (Fig. 7).

3.3. The influence of hydrological factors on tree-ring growth

3.3.1. Correlation analysis

At Bracciano, water-level fluctuations showed a strong influence on tree-ring growth, as expected. Significant correlations were found at each timescale and for all variables included in the analysis. However, the highest significant correlation coefficients were found with monthly and seasonal variables (three and six months), while on a yearly scale, the influence of WL decreased with an increase in the number of preceding years, disappearing at year $t + t_{-5}$ (Fig. 8).

The intra-annual WL has raisen during spring and then dropped, reaching the minimum values in autumn–early winter (Fig. 8). At the monthly scale, the highest correlations were found from September to December of the previous year and from September to November of the current year.

For the period of 2007–2016, tree-ring growth showed significant correlations at the yearly scale with lake evaporation, water withdrawal (negative) and water reservoir (positive), especially when including the effect of the previous year (Table 5). TRW produced more significant correlations (Spearman, ρ) than BAI, with the highest coefficients occurring when correlated with water reservoir (0.87, $p < .01$) and water withdrawal (-0.83, $p < .01$) when including the effect of the previous year, as well as lake evaporation (-0.87, $p < .01$). BAI chronology produced a similar correlation pattern except for with water withdrawal, which slightly influenced BAI only when including the previous year's effect (-0.65, $p = .05$).

3.3.2. PLSR analysis

According to the PLSR analysis shown in Fig. 9 (including the VIP; Fig. 9b), seasonal SPEI and precipitation (NDj and SONDjf) and water reservoir accumulated from the previous year (WR[$t + t_{-1}$]) were highly correlated with RWI chronology. The effect of P and SPEI of the previous year (P[$t + t_{-1}$] and SPEI[$t + t_{-1}$]) and monthly (November) water levels (WL.n) of the current year also showed a significant influence on RWI. On the contrary, lake evaporation followed by water withdrawal, especially when including the effect of the previous year (E[$t + t_{-1}$] and WW[$t + t_{-1}$], respectively), were the main independent variables negatively correlated with RWI chronology. The model explained more than 92% of the tree-ring growth variability and showed high goodness of prediction ($Q^2 = 0.73$; Fig. 9c). Furthermore, the RMSECV was very low (1.81%) and the RPD was 5.10.

3.4. The influence of water-level fluctuations on growth dynamics

The relative growth change method characterized the 1991, 2003 and 2017 years as negative pointer years, which coincide with some of the lowest annual water levels below the 10^{th} (1991) and 5^{th} (2003, 2017) percentile (Fig. 10a). The percentage of trees showing the negative pointer years in these critical years were 78, 88 and 88 %, respectively.

Resistance (Rt) indices clearly revealed a strong growth reduction during the critical water levels occurred in 1991, 2003 and 2017 (39.5, 58. 5 and 54.5 %, respectively), but no significant differences were found. Resilience (Rs) indices revealed lower growth levels compared to

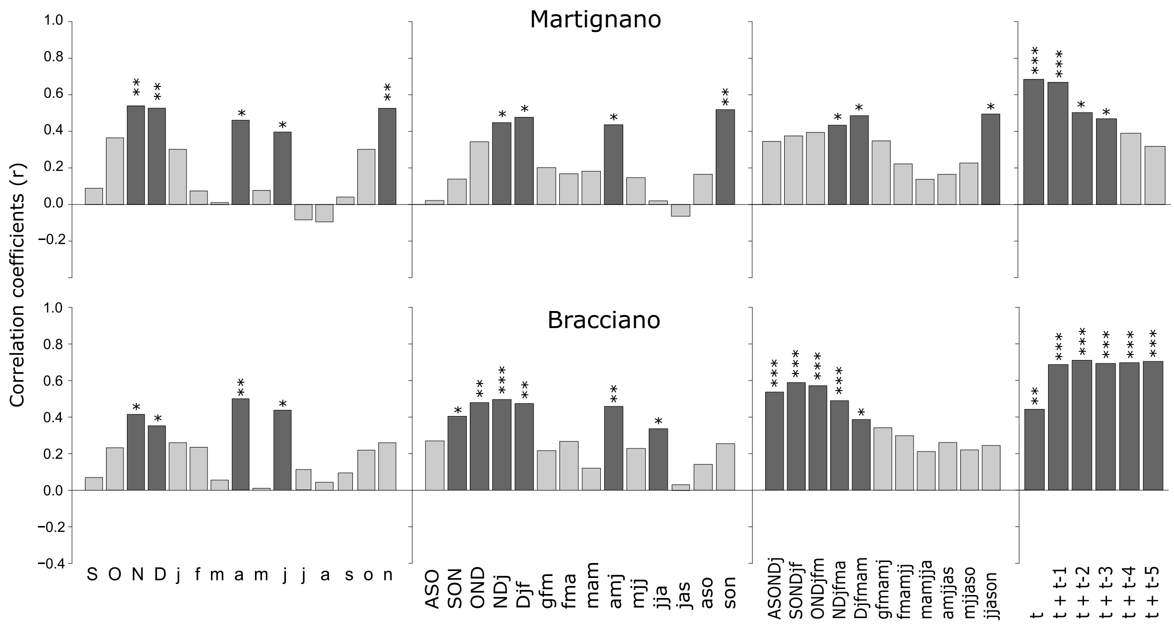

Figure 5. Pearson's correlation coefficients between standardised tree-ring whidth chronologies (RWI) and precipitation variables at monthly, seasonal and yearly scales. Lowercase and uppercase letters refer to the current year of growth and the year before, respectively. Yearly variables include values up to five years prior to the current year of tree-ring formation: $t + t_{-i}$, where t is the value of the current year and i ranges from 1 to 5. The dark bar charts indicate significant values. * $p < .05$; ** $p < .01$; *** $p < .001$.

those 3 years before the critical water levels. Moreover, the growth level reduction was significantly greater in 2003 than in 1991 (42.0 vs. 23.2 %, $p < .05$) (Fig. 10b).

The recovery (Rc) indices revealed a contrasting pattern in the ability to recover growth level after the reduction experienced during disturbances (critical water levels) occurred in 1991 and 2003. Tree ring growth recovery after the critical year 1991 was higher in the long-term (from 6 to 9 years, 57.1 vs. 41.3 % on average), while after the 2003 in the short-term (from 3 to 5 years, 30.2 vs. 41.5 % on average) (Fig. 10b).

4. Discussion

4.1. Growth responses to climatic drivers

Riparian trees show common adaptive traits such as the rapid root extension and low shoot-to-root biomass ratios, which potentially reduce stress related to seasonally variable water tables (Kranjcec et al., 1998; Amlin and Rood, 2002). The common phreatophitic behaviour most likely produced the highly significant synchrony among species at the site level. Consequently, we combined the three riparian species within each site to find a pattern in climate-growth relationships

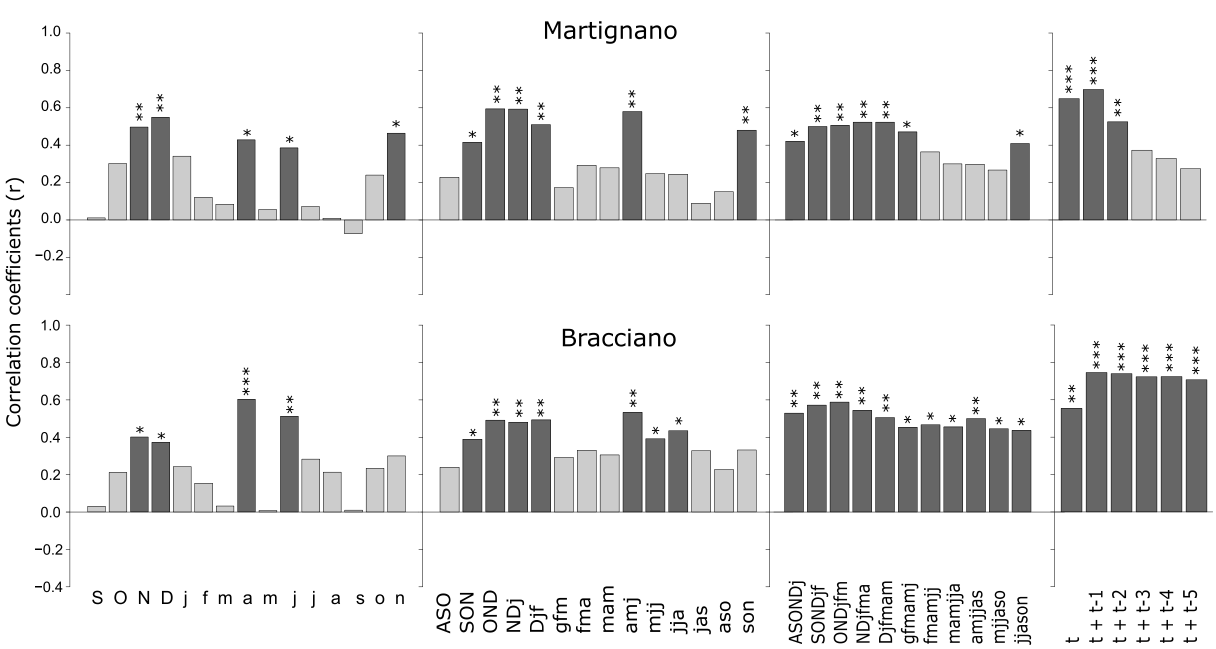

Figure 6. Pearson's correlation coefficients between RWI and SPEI variables at monthly, seasonal and yearly scales. See Figure 5 for x-axis labels. The dark bar charts indicate significant values. * $p < .05$; ** $p < .01$; *** $p < .001$.

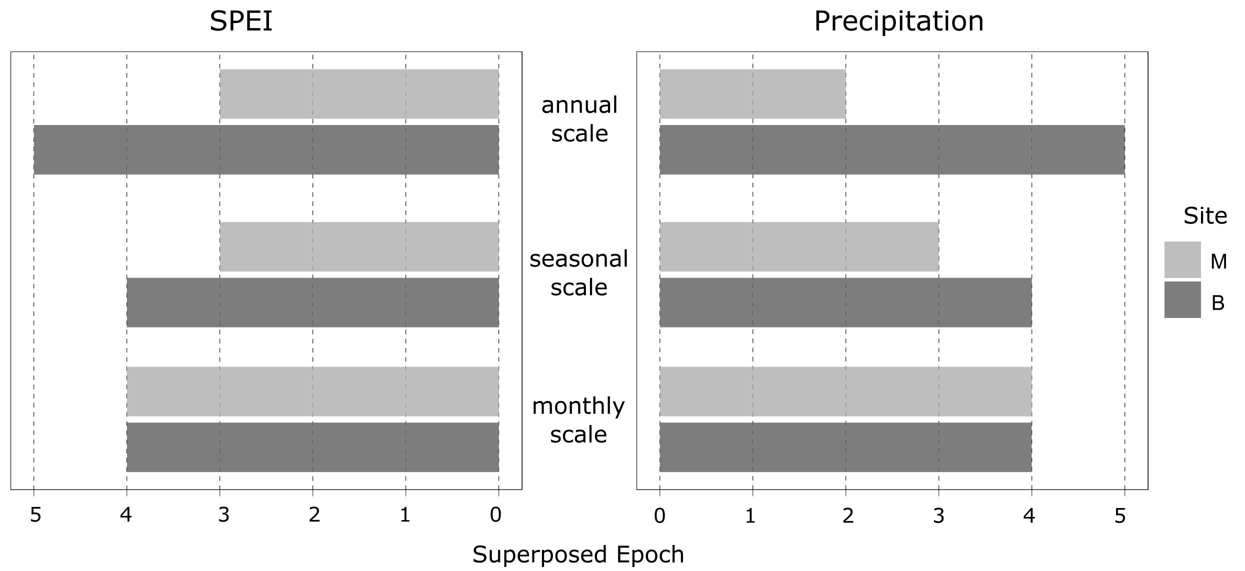

Figure 7. Superposed epoch analysis (SEA) results showing the significant influence ($p < .05$) of severe drought events on tree-ring growth reduction during the drought years (0) and the years after the drought (1 to 5) at monthly, seasonal and annual scale. For each time scale, the SEA results of all the significant climatic variables as resulting from the climate-growth correlation analysis (Figs. 5 and 6) were combined.

potentially related to the different disturbance regimes (the human water use at Bracciano), discriminating against the two sites. Other studies reported higher synchrony and stronger correlations between the master site chronology and the main climatic predictors of tree ring growth than mean curves of the individual species (e.g., Worbes, 1999; Schöngart et al., 2006; Gebrekirstos et al., 2008).

The drought-driven decrease in tree growth over the last years appeared more significant for Bracciano chronology, although from the end of the 2000s, a steep decrease was also observed in the Martignano chronology.

Overall, comparing growth responses to precipitation of the two lakes' riparian vegetation at monthly to seasonal time scales (short climatic signals), the main contrasting pattern was the significant influence on tree-ring growth of November and autumn of the current year only at Martignano. On the other hand, the influence of previous precipitation (e.g. late summer – autumn) on tree-ring growth was more significant at Bracciano than Martignano. The greater human impact on the Bracciano lake (i.e., the water withdrawal by the water management agency of Rome – ACEA, the presence of surrounding municipalities and infrastructures for touristic activities along the shoreline) most likely influenced the water level drop, increasing the groundwater flow to the lake and allowing trees to be more dependent on groundwater rising or soil water content stored from the previous rainy periods (e.g. three and six months). This distinctive pattern in climate-growth relationships appeared clearer when increasing the timescale of climatic drivers up to multiple years of precipitation (long-term signals, Figure 5). On the other hand, trees from Martignano riparian vegetation can utilise the groundwater rise after the summer drought due to the current autumn precipitation. As the groundwater is strictly related to WL fluctuations, at Bracciano the coupled effect of summer drought and water withdrawal (absent at Martignano) cause minimum WL values in autumn, slowing down the groundwater recharge during the autumn months.

Therefore, precipitation accumulated over not only consecutive

Table 5
Spearman correlation coefficients (ρ) between standardized tree-ring widths (RWI) and the main hydrological variables of the lake-water balance: lake evaporation (E), water reservoir (WR) and water withdrawal (WW) of the current year (t) and including the effect of the previous year ($t+t_{-1}$).

Variables	Acronym	ρ
Annual lake evaporation	E(t)	-0.87**
2-years lake evaporation	$E(t+t_{-1})$	-0.81*
Annual water reservoir	WR(t)	-
2-years water reservoir	$WR(t+t_{-1})$	0.87**
Annual water withdrawal	WW(t)	- 0.65*
2-years water withdrawal	$WW(t+t_{-1})$	- 0.83**

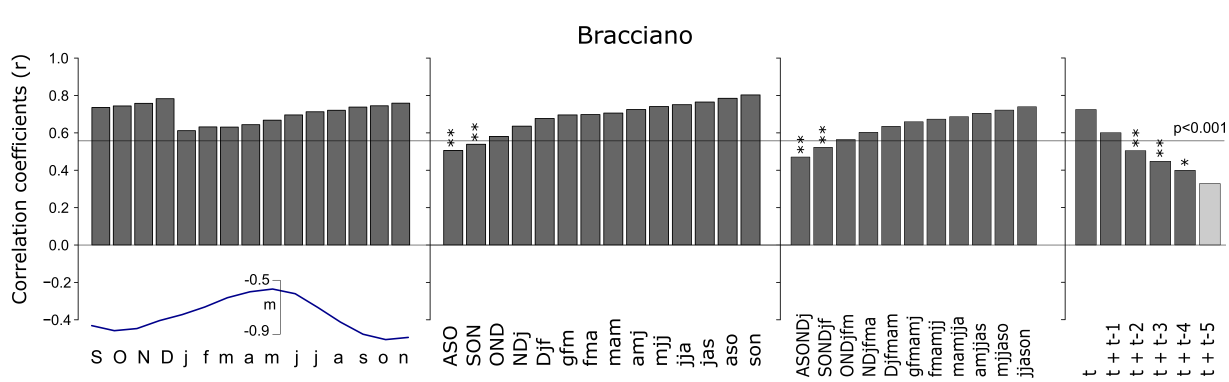

Figure 8. Pearson's correlation coefficients between RWI and water-level (WL) variables at monthly, seasonal and yearly scales. See Figure 5 for x-axis labels. The dark bar charts indicate significant values. * $p < .05$; ** $p < .01$; horizontal continuous line $p < .001$. Mean intra-annual water-level fluctuations (m) are also provided.

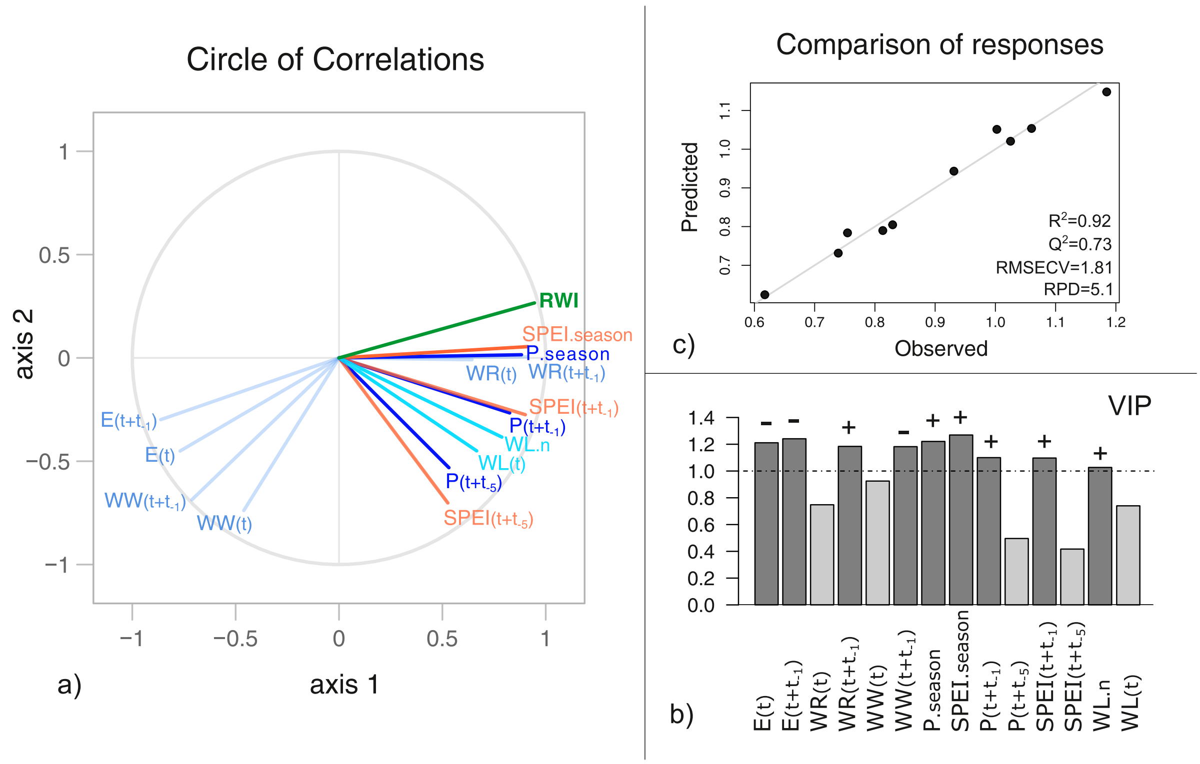

Figure 9. Partial least squares regression (PLSR) analysis, showing the correlations between the selected hydroclimatic factors and RWI. Box a) Circle of correlations of the first two components. P: precipitation; SPEI; E: mean annual lake evaporation; WR: water reservoir; WW: ACEA Spa (water management agency of Rome) direct water withdrawal. Box b) VIP: variable influence on projection of each predictor. Only predictors with VIP > 1 are considered of significant importance for the prediction. Signs (+ and -) indicate the trend of regression parameters. Box c) Comparison between observed RWI and predictions made by PLSR model. R^2 is the goodness-of-fit for all observations; Q^2 stands for cross-validated goodness of prediction (with two PLSR components), RMSECV is the root mean square error of cross-validation and RPD is the residual predictive deviation.

months, but also consecutive years, most likely plays an important role in groundwater rising, allowing trees to reach this water reserve with their deepest roots. For *A. glutinosa*, for example, it was reported that roots can reach almost 5 m deep (Claessens et al., 2010).

The influence of drought on tree-ring growth confirmed the distinctive pattern in climate-growth correlations produced by SPEI variables especially on an annual scale, suggesting a cumulative stress effect. Moreover, results for SPEI pattern highlighted the role of drought as a limiting factor during the summer.

According to a groundwater/surface water model (Taviani and Henriksen, 2015) developed to test the vulnerability of Bracciano Lake to climatic and water-use stresses, when dry conditions were simulated over a long time period by imposing a stable decrease in recharge and net precipitation, the simulated average lake level dropped sharply. The wavelet analysis confirmed this pattern, showing an increasing dependence of WL on precipitation and SPEI when increasing the frequency

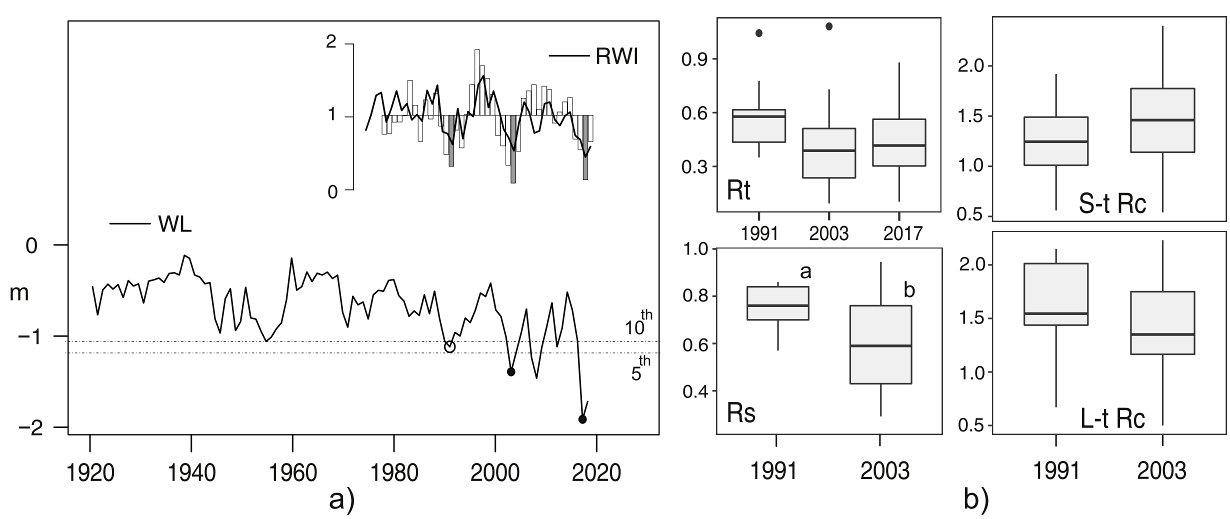

Figure 10. a) Water-level (WL) fluctuations and ring-width index RWI at the Bracciano site. The overlapped barplot indicates the mean annual growth deviation (in percentage) with negative pointer years in grey fill color (1991, 2003 and 2017). Open and full circles indicate critical water levels below the 10^{th} and 5^{th} percentile, respectively. b) Resistance (Rt), resilience (Rs) and Recovery (Rc) indices calculated from TRW for the mean site chronology of Bracciano. Rc was calculated as short-term (S-t, from 3 to 5 years) and long-term (L-t, from 6 to 9 years) recovery after the critical water levels occurred in 1991 and 2003.

band-pass (long-term signals, Table 4).

Based on the hydrogeological model of Bracciano Lake with a water budget dominated by net precipitation flux, the simulated dry conditions in the short term were slightly balanced by the increased net groundwater flow to the lake during summer months (Taviani and Henriksen, 2015). This suggested that prolonged dry conditions decreased the groundwater availability for riparian vegetation, especially during the summer period.

The highest significant correlations of precipitation accumulated over consecutive previous years with tree-ring growth can suggest that environmental conditions in previous years are a determining factor in the ability of trees to overcome the negative effects of drought on growth (Sarris et al., 2011; Mazza et al., 2014; Ogle et al., 2015; Johnstone et al., 2016; Peltier et al., 2017; Mazza and Sarris, 2018).

According to the partial least square regression analysis, the climatic drivers were the main predictors influencing tree-ring growth. Indeed, focusing only on predictors with VIP values >1, SPEI and precipitation were the most significant independent variables. The strong influence of SPEI on tree-ring growth is probably due to the integration of different climate conditions (temperature, rainfall and evapotranspiration) into a single variable.

4.2. The influence of hydrological factors on tree-ring growth

At Bracciano, the water-level fluctuations showed a strong influence on tree-ring growth as independent variables. They were highly significant for each combination of predictors for each timescale included in the correlation analysis. Contrary to precipitation and SPEI, water-level variables were mainly correlated with tree-ring growth at monthly and seasonal scales, suggesting a high sensitivity of riparian vegetation tree-ring growth to short-term water-level fluctuations, especially during their minimum intra-annual values (autumn–early winter) (see Fig 8). Indeed, it was observed that when the water level drops, both lakes draw water from the groundwater also in the short term. In a river basin in southern Portugal, September and November discharge reduced resilience (considering both BAI and raw ring width) of coexisting *Alnus glutinosa* and *Fraxinus angustifolia* (Gomes Marques et al., 2018). The significant positive correlations between tree-ring growth and water level during the maximum recharge (from late winter to late spring) could be related to the replenishment of the lake water reservoir, allowing trees to sustain drought events, as also found by Gomes Marques et at. (2018).

Including WL variables in the partial least square regression models, revealed a lower predictive power compared to the other independent variables. Based on VIP values >1, the main hydrological predictor influencing tree-ring growth was lake evaporation (negative), followed by water reservoir (positive) and water withdrawal (negative) when including the previous year's values. This result is in line with the Bracciano lake water balance, according to which the most important outflows from the lake are evaporation from the surface and withdrawals for water supply, estimated to be 0.985 m/year (1.78 m^3/s) and 0.166 m/year (0.3 m^3/s) respectively (Taviani and Henriksen, 2015).

Our results suggested that local hydrology conditions were essential for tree growth of riparian vegetation due to its position closer to the lake and its relative protection from climate extremes such as high temperatures and water stress—typical features of wetland tree species. This is in line with the general hypothesis that both climate and site-specific conditions driving water availability would strongly shape environmental signals retained in riparian tree-ring widths (Rodríguez-González et al., 2014; Koprowski et al., 2018). Indeed, riparian species are very sensitive to the reduction in water resources availability (e.g. water table drop) because they rely on a phreatophytic root morphology, with deep roots permanently accessing groundwater or the stream (Singer et al., 2013).

Moreover, although the riparian species sampled were diffuse-porous, thus presumably less susceptible to cavitation than ring-porous species, their roots can be vulnerable to drought (Hacke and Sauter, 1996) due the little ability of phreatophytes to regulate transpirational water loss (Johnson et al., 2002). There is evidence that stomata react to information about the soil water status mediated by metabolic signals from the roots (Zhang et al., 1987; Eschenbach and Kappen, 1999; Xu et al., 2018). The increase in drought conditions during the summer period could reduce tree ring growth due to water loss by evapotranspiration, making this more evident for trees that experienced a significant groundwater level drop caused by intense water withdrawals over the last years. Indeed, during dry and hot periods such as the typical Mediterranean summer, transpiration of the riparian tree species is mostly supported by the access to the phreatic water table. However, if lake water level drops the phreatic water table might descend below the rooting depth, uncoupling the riparian trees from such extra water (Nadal-Sala et al., 2017). A similar condition can occur when the water level drop increases the groundwater inflow to the lake, as observed at Bracciano (Taviani and Henriksen, 2015). Losing contact with the groundwater reserve, tree water uptake capacity is linked directly to the unsaturated soil water availability, and it makes trees decrease carbon uptake, reducing growth. Thus, when the deeper roots cannot access phreatic water (e.g. during droughts), lower rates of water uptake by the shallow roots from a moderately small pool of unsaturated soil water cannot satisfy canopy demand and thus induce stress on riparian tree species, which considerably decreases growth (Singer et al., 2013).

4.3. WL effect on growth dynamics

A decreasing trend in Bracciano water-level fluctuations was evident, especially after the late 1970s (Fig. 10a). Despite the relatively large volume of Bracciano Lake buffering the effects of water withdrawal and making the water depletion less evident, the drawdown of 0.5 m recorded over the last 50 years corresponded to the total loss of water from the lake of around 28 Mm^3 (Taviani and Henriksen, 2015). As expected, the impact of lake water level drop on riparian woody vegetation growth pattern and dynamics was well recorded in tree-rings widths (Fig. 10a). When the first critical water level occurred (in 1991), the ability of tree ring growth to sustain stress conditions (resistance) was less affected compared to other two critical years (2003 and 2017). According to definitions in Lloret et al. (2011), it means that the significant water level drop in 1991 had less impact on “the reduction in ecological performance during disturbance”. Similarly, the capacity to recover from disturbance and reach pre-disturbance levels (resilience) showed the same pattern and was significantly higher in 1991 than 2003.

On the other hand, the capacity to recover from the damage experienced in a particular critical year showed a contrasting pattern between 1991 and 2003. After 2003 the tree ring growth recovery was significant only in the short-term, while after 1991 it lasted longer. It can suggest a greater capacity to recover in the long-term the growth reduction experienced in 1991. Indeed, when water level drop occurred in 1991, the previous drought conditions increased only considering the cumulative effect over 3-4 consecutive years but were always less dry than 2003 and 2017.

In addition to the years 1991, 2003 and 2017, the lake water level drop occurred in 2008 was also significant (below the 5^{th} percentile). Nevertheless, it did not cause significant negative growth changes. Contrary to 2003 and 2017, the year 2008 was characterized by greater annual precipitation compared to the previous year as well as to that accumulated up to 4 years before. Similarly, during 2008 did not occur severe drought conditions, expressed by SPEI, as the previous years.

Pre-disturbance climatic conditions (e.g. drought increase) affect the vulnerability of trees to later disturbing events (e.g. critical lake water levels), influencing their capacity to recover from disturbance and reach pre-disturbance growth levels. Preceding and prolonged climatic conditions that are physiologically stressful can increase disturbance-induced tree-ring growth decrease and reduce its subsequent recovery capacity (Johnstone et al., 2016).

Riparian trees species are well adapted to the seasonality of water-level variations as a typical feature of their habitats (Stella et al., 2013). Changes in disturbance regimes (e.g. disturbance frequency, severity, or timing) can modify patterns and processes of recovery, which in turn depend on the contemporary environment and the persistent effects, or legacies, of past events (Franklin et al., 2000; Seidl et al., 2014; Monger et al., 2015; Johnstone et al., 2016).

5. Conclusion

Our study based on a dendroecological analysis of riparian trees vegetation suggested a helpful approach both to improve the understanding of climate variability effects on tree ring growth and to detect a range of critical water-level thresholds affecting tree resilience and growth recovery.

By studying two riparian forest ecosystems growing under different disturbance regimes (mainly related to human water use), we highlighted some distinctive key points in growth responses to climate variability. The short- to long-term shifting in climatic factors significantly correlated with tree-ring growth could be a human-induced modification in the water resources recharging, strictly related to withdrawals for public supply. At Bracciano the most important water inflow is from precipitation directly on the lake, therefore prolonged reduction of precipitation input may leave it sensitive to climate change and water withdrawals. Thus, the overexploitation of water resources for public water supply, agriculture, tourism, or other needs may increase trees' vulnerability to predicted drought intensification effects.

Based on our results, we hypothesized that the water levels ranging between the two critical years 1991 and 2003 (-108 and -139 cm, respectively) may be considered as potential thresholds affecting riparian tree growth in the study sites. Consequently, this information may support a reasonable lake water withdrawal management and regulation, and would be helpful for riparian woody vegetation protection, favouring the persistence of their ecological and functional features.

Declaration of competing interests

The authors declare that they have no known competing financial interests or personal relationships that could have appeared to influence the work reported in this paper.

Acknowledgments

This work was supported by the Project “DendroRiparian”, funded by the Regional Natural Park of Bracciano-Martignano (Lazio region, Italy). The authors would like to thank the Director and the personnel from Regional Natural Park of Bracciano-Martignano for lake water-level data, field assistance and collaboration. We are grateful to the hydrogeologist Alessandro Mecali for his useful suggestions. We also wish to thank two anonymous reviewers for their useful comments and suggestions that helped to improve the article.

Supplementary materials

Supplementary material associated with this article can be found, in the online version, at doi:10.1016/j.agrformet.2020.108036.

References

Allen, S.J., Hall, R.S., Rosier, P.T.W., 1999. Transpiration by two poplar varieties grown as coppice for biomass production. Tree Physiol 19, 493–501.

Amlin, N.M., Rood, S.B., 2003. Drought stress and recovery of riparian cottonwoods due to water table alteration along Willow Creek, Alberta. Trees Struct. Funct 17 (4), 351–358.

Adrian, R., O'Reilly, C.M., Zagarese, H., Baines, S.B., Hessen, D.O., Keller, W., et al., 2009. . Lakes as sentinels of climate change. Limnol Oceanogr 54 (6), 2283–2297. PMID:20396409.

Bégin, Y., 2001. Tree-Ring Dating of Extreme Lake Levels at the Subarctic–Boreal Interface. Quat. Res. 55 (2), 133–139. https://doi.org/10.1006/qres.2000.2203.

Blasi, C., 1994. Fitoclimatologia del Lazio. Fitosociologia 27, 151–175.

Boni, M.R., Rossi, A., D'Amato, E., Sappa, G., Ferranti, F., 2017. Il lago di Bracciano come risorsa idropotabili: gli aspetti ecologici e idrogeologici. Conseguenze ambientali dovute al mantenimento dei prelievi. Report preliminare. Pp. 57.

Brunetti, M., Maugeri, M., Monti, F., Nanni, T., 2006. Temperature and precipitation in Italy in the last two centuries from homogenised instrumental time series. Int. J. Climatol. 26, 345–381.

Bunn, A.G., 2008. A dendrochronology program library in R (dplR). Dendrochronologia 26, 115–124.

Bunn, A.G., 2010. Statistical and visual crossdating in R using the dplR library. Dendrochronologia 28 (4), 251–258.

Buras, A., Wilmking, M., 2015. Correcting the calculation of Gleichläufigkeit. Dendrochronologia 34, 29–30. https://doi.org/10.1016/j.dendro.2015.03.003.

Carrascal, L.M., Galván, I., Gordo, O., 2009. Partial least squares regression as an alternative to current regression methods used in ecology. Oikos 118, 681–690.

Claessens, H., Oosterbaan, A., Savill, P., Rondeux, J., 2010. A review of the characteristics of black alder (*Alnus glutinosa* (L.) Gaertn.) and their implications for silvicultural practices. Forestry 83, 163–175.

Cook, E.R., Kairiukstis, L.A., 1990. Methods of Dendrochronology: Applications in Environmental Science. Kluwer Academic PublishersSpringer, Doredrecht, NetherlandsNetherlands, pp. 394 ISBN 0-7923-0586-8.

Cox, G., Fischer, D., Hart, S., Whitham, T.G., 2005. Non-response of native cottonwood trees to water additions during summer drought. West. N. Am. Natural. 65, 175–185.

Crisman, T.L., Mitraki, C., Zalidis, G., 2005. Integrating vertical and horizontal approaches for management of shallow lakes and wetlands. Ecol. Eng. 24, 379–389.

Dufour, S., Piégay, H., 2008. Geomorphological controls of *Fraxinus excelsior* growth and regeneration in floodplain forests. Ecology 89 (1), 205–215.

Elliott, K.J., Miniat, C.F., Pederson, N., Laseter, S.H., 2015. Forest tree growth response to hydroclimatic variability in the southern Appalachians. Global Change Biol 21, 4627–4641. https://doi.org/10.1111/gcb.13045.

Eschenbach, C., Kappen, L., 1999. Leaf water relations of black alder (*Alnus glutinosa* [L.] Gaertn.) growing at neighbouring sites with different water regimes. Trees 14, 28–38.

Fearn, T., 2002. Assessing calibrations: SEP, RPD, RER and R2. NIR News 13 (6), 12–13.

Franklin, J.F., Lindenmayer, D.B., MacMahon, J.A., McKee, A., Magnuson, J., Perry, D.A., Waide, R., Foster, D., 2000. Threads of continuity. Conserv. Biol. Pract. 1, 8–16.

Fritts, H.C., 1976. Tree rings and climate. Academic, San Diego, California, pp. 567.

Gärtner, H., Nievergelt, D., 2010. The core-microtome. A new tool for surface preparation on cores and time series analysis of varying cell parameters. Dendrochronologia 28, 85–92. https://doi.org/10.1016/j.dendro.2009.09.002.

Gärtner, H., Banzer, L., Schneider, L., Schweingruber, F., Bast, A., 2015. Preparing micro sections of entire (dry) conifer increment cores for wood anatomical time-series analyses. Dendrochronologia 34, 19–23. https://doi.org/10.1016/j.dendro.2015.03.004.

Gebrekirstos, A., Mitlöhner, R., Teketay, D, Worbes, M., 2008. Climate-growth relationships of the dominant tree species from semi-arid savanna woodland in Ethiopia. Trees 22, 631–641.

Ghil, M., Allen, M.R., Dettinger, M.D., Ide, K., Kondrashov, D., Mann, M.E., Robertson, A.W., Saunders, A., Tian, Y., Varadi, F., Yiou, P., 2002. Advanced spectral methods for climatic time series. Rev. Geophys 40 (1), 1–41. https://doi.org/10.1029/2000RG000092. 2002.

Gomes Marques, I., Campelo, F., Rivaes, R., Albuquerque, A., Ferreira, M.T., Rodriguez-Gonzalez, P.M., 2018. Tree rings reveal long-term changes in growth resilience in Southern European riparian forests. Dendrochronologia 52, 167–176.

Gownaris, N.J., Rountos, K.J., Kaufman, L., Kolding, J., Lwiza, K.M.M., Pikitch, E.K., 2018. Water level fluctuations and the ecosystem functioning of lakes. J. Great Lakes Res. 44, 1154–1163. https://doi.org/10.1016/j.jglr.2018.08.005.

Grissino-Mayer, H.D., 1993. An updated list of species used in tree-ring research. Tree Ring Bull 53, 17–43.

Gunderson, L.H., 2000. Ecological resilience — in theory and aplication. Annu. Rev. Ecol. Syst. 31, 425–439. https://doi.org/10.1146/annurev.ecolsys.31.1.425.

Hacke, U., Sauter, J.J., 1996. Drought-induced xylem dysfunction in petioles, branches and roots of *Populus balsamifera* L. and *Alnus glutinosa* (L.) Gaertn. Plant Physiol 111, 413–417.

Hair, J.F., Hult, G.T.M., Ringle, C.M., Sarstedt, M., 2017. A Primer on Partial Least Squares Structural Equation Modeling (PLS-SEM), 2nd ed. Sage, Thousand Oaks, CA.

Hamed, K.H., 2008. Trend detection in hydrologic data: the Mann–Kendall trend test under the scaling hypothesis. J. Hydrol. 349, 350–363.

Harrington, C.A., Curtis, R.O., 1986. Height growth and site index curves for red alder. Pacific Northwest Research Station, USDA Forest Service Research Paper.

IPCC, 2007. Climate Change 2007: Impacts, Adaptation and Vulnerability. Contribution of Working Group II to the Fourth Assessment Report of the Intergovernmental Panel on Climate Change. In: Parry, M.L., Canziani, O.F., Palutikof, J.P., van der Linden, P.J., Hanson, C.E. (Eds.), Cambridge University Press, Cambridge, UK, pp. 7–22.

IUSS Working Group WRB.2015. World Reference Base for Soil Resources 2014, update 2015 International soil classification system for naming soils and creating legends for soil maps. World Soil Resources Reports No. 106. FAO, Rome.

Johnson, J., Tognetti, R., Paris, P., 2002. Water relations and gas exchange in poplar and willow under water stress and elevated atmospheric CO_2. Physiol. Plantarum. 115, 93–100. https://doi.org/10.1034/j.1399-3054.2002.1150111.x.

Johnstone, J.F., Allen, C.D., Franklin, J.F., Frelich, L.E., Harvey, B.J., Higuera, P.E., Mack, M.C., Meentemeyer, R.K., Metz, M.R., Perry, G.L., Schoennagel, T., Turner, M.G., 2016. Changing disturbance regimes, ecological memory, and forest resilience. Front. Ecol. Environ. 14, 369–378. https://doi.org/10.1002/fee.1311.

Koprowski, M., Okoński, B., Gričar, J., Puchałka, R., 2018. Streamflow as an ecological factor influencing radial growth of European ash (*Fraxinus excelsior* (L.)). Ecol. Indic 85, 390–399. https://doi.org/10.1016/j.ecolind.2017.09.051.

Kranjcec, J., Mahoney, J.M., Rood, S.B., 1998. The responses of three riparian cottonwood species to water table decline. For. Ecol. Manage. 110, 77–87.

Lloret, F., Keeling, E.G., Sala, A., 2011. Components of tree resilience: effects of successive low-growth episodes in old ponderosa pine forests. Oikos 120, 1909–1920. https://doi.org/10.1111/j.1600-0706.2011.19372.x.

Lowry, P.B., Gaskin, J., 2014. Partial least squares (PLS) structural equation modeling (SEM) for building and testing behavioral causal theory: When to choose it and how to use it. IEEE Trans. Prof. Commun. 57, 123–146.

Marqués, L., Camarero, J.J., Gazol, A., Zavala, M.A., 2016. Drought impacts on tree growth of two pine species along an altitudinal gradient and their use as early-warning signals of potential shifts in tree species distributions. For. Ecol. Manage 381, 157–167.

Mazza, G., Cutini, A., Manetti, M.C., 2014. Influence of tree density on climate-growth relationships in a *Pinus pinaster* Ait. forest in the northern mountains of Sardinia (Italy). iForest8 (4), 456–463.

Mazza, G., Sarris, D., 2018. The influence of low-frequency variability on tree-rings based climate reconstruction: a case study from central Italy (Roman coast). Ann. Silvic. Res. 42 (2), 68–78.

Merritt, D.M., Scott, M.L., LeRoy, P., Auble, G.T., Lytle, D.A., 2010. Theory, methods and tools for determining environmental flows for riparian vegetation: Riparian vegetation-flow response guilds. Freshw. Biol. 55, 206–225. https://doi.org/10.1111/j.1365-2427.2009.

Monger, C., Sala, O.E., Duniway, M.C., Goldfus, H., Meir, I.A., Poch, R.M., Throop, H., Vivoni, E., 2015. Legacy effects in linked ecological-soil- geomorphic systems of drylands. Front. Ecol. Environ. 13, 13–19. https://doi.org/10.1890/140269.

Nadal-Sala, D., Sabaté, S., Sánchez-Costa, E., Poblador, S., Sabater, F., C. Gracia, C., 2017. Growth and water use performance of four co-occurring riparian tree species in a Mediterranean riparian forest. For. Ecol. Manage. 396, 132–142.

Naiman, R.J., Décamps, H., McClain, M.E., 2010. Riparia: Ecology, conservation, and management of streamside communities. London, UK: Academic Press.

Napoli, R., Paolanti, M., Rivieccio, R., Di Ferdinando, S., 2019. Carta dei suoli del Lazio in Scala 1:250.000 ARSIAL Regione Lazio. ISBN 978-88-904841-2-4.

Naselli-Flores, L., Barone, R., 2005. Water–level fluctuations in Mediterranean reservoirs: Setting a dewatering threshold as a management tool to improve water quality. Hydrobiologia 548, 85–99.

Netsvetov, M., Prokopuk, Y., Puchałka, R., Koprowski, M., Klisz, M., Romenskyy, M., 2019. River Regulation Causes Rapid Changes in Relationships Between Floodplain Oak Growth and Environmental Variables. Front. Plant Sci. 10, 96. https://doi.org/10.3389/fpls.2019.00096.

Ogle, K., Jarrett, J.B., Barron-Gafford, G.A., Bentley, L.P., Young, J.M., Travis, E.H., Loik, M.E., Tissue, D.T., 2015. Quantifying ecological memory in plant and ecosystem processes. Ecol. Lett. 18, 221–235.

Papastergiadou, E., Kagalou, I., Stefanidis, K., Retalis, A., Leonardos, I., 2010. Effects of Anthropogenic Influences on the Trophic State, Land Uses and Aquatic Vegetation in a Shallow Mediterranean Lake: Implications for Restoration. Water Resour. Manag 24, 415–435.

Paulo, J.A., Palma, J.H.N., Gomes, A., Faias, S., Tomé, J., Tomé, M., 2015. Predicting site index from climate and soil variables for cork oak (*Quercus suber* L.) stands in Portugal. New For 46 (2), 293–307. https://doi.org/10.1007/s11056-014-9462-4.

Peltier, D.M.P., Barber, J.J., Ogle, K., 2017. Quantifying antecedent climatic drivers of tree growth in the Southwestern US. J. Ecol. 00, 1–12.

Percival, D.B., Walden, A.T., 2000. Wavelet Methods for Time Series Analysis. Cambridge Univ. Press, Cambridge, UK.

Perneger, T.V., 1998. What's wrong with Bonferroni adjustments. Br. Med. J. 316, 1236–1238.

R Core Team, 2019. R: A Language and Environment for Statistical Computing. Foundation for Statistical Computing, Vienna, Austria ([online] URL). http://www.r-project.org.

Rains, M.C., Mount, J.E., Larsen, E.W., 2004. Simulated changes in shallow groundwater and vegetation distributions under different reservoir operations scenarios. Ecol. Appl. 14 (1), 192–207.

Rinn, F., 2012. TSAP-Win Professional, Time Series Analysis and Presentation for Dendrochronology and Related Applications, Version 4.6x for Microsoft Windows, Quick Reference, Vol. 20. Rinntech, Heidelberg.

Rodríguez-González, P.M., Campelo, F., Albuquerque, A., Rivaes, R., Ferreira, M.T., Santos Pereira, J., 2014. Sensitivity of black alder (*Alnus glutinosa* [L.] Gaertn.) growth to hydrological changes in wetland forests at the rear edge of the species distribution. Plant Ecol 215 (2), 233–245. https://doi.org/10.1007/s11258-013-0292-9.

Sarris, D., Christodoulakis, D., Korner, C., 2011. Impact of recent climatic change on growth of low elevation eastern Mediterranean forest trees. Clim. Change 106 (2), 203–223.

Schöngart, J., Orthmann, B., Hennenberg, K.J., Porembski, S., Worbes, M., 2006. Climate–growth relationships of tropical tree species in West Africa and their potential for climate reconstruction. Glob. Chang Biol. 12, 1139–1150.

Schweingruber, F.H., Eckstein, D., Serre-Bachet, F., Bräker, O.U., 1990. Identification, presentation and interpretation of event years and pointer years in dendrochronology. Dendrochronologia 38, 8–9.

Seidl, R., Rammer, W., Spies, T.A., 2014. Disturbance legacies increase the resilience of forest ecosystem structure, composition, and functioning. Ecol. Appl. 24, 2063–2077.

Seiwa, K., Kikuzava, K., Kadowaki, T., Akasakxa, S., Naoto, U., 2005. Shoot life span in relation to successional status in deciduous broad-leaved tree species in a temperate forest. New Phytol 169, 537–548.

Singer, M., Stella, J., Dufour, S., Piégay, H., Wilson, R.J.S., Johnstone, L., 2013. Contrasting water uptake and growth responses to drought in co-occurring riparian tree species. Ecohydrology 6, 402–412.

Snyder, K.A., Williams, D.G., 2007. Root allocation and water uptake patterns in riparian tree saplings: Responses to irrigation and defoliation. For. Ecol. Manage. 246 (2–3), 222–231.

Stella, J., Rodríguez-González, P.M., Dufour, S., Bendix, J., 2013. Riparian vegetation research in Mediterranean-climate regions: Common patterns, ecological processes, and considerations for management. Hydrobiologia 719 (1), 291–315. https://doi.org/10.1007/s10750-012-1304-9.

Stockton, C.W., Fritts, H.C., 1973. Long-term reconstruction of water level changes for Lake Athabaska by analysis of tree-rings. Water Resour. Bull. 9, 1006–1027. https://doi.org/10.1111/j.1752-1688.1973.tb05826.x.

Taviani, S., Henriksen, H.J., 2015. The application of a groundwater/surface model to test the vulnerability of a deep lake in the vicinity of Roma, Italy to climatic and water use stresses. Hydrogeol. J 23 (7), 1481–1498.

Tenenhaus, M., 1998. La régression PLS - Théorie et pratique. Editions Technip, Paris.

Thibaut, A., Rondeux, J., Claessens, H., 2004. Site index curves for *Alnus glutinosa* (L.) Gaertn.] in Southern Belgium: effect of site on the curve shape. Forestry 77 (2), 157–171.

Torrence, C., Compo, G.P., 1998. A practical guide to wavelet analysis. Bull. Am. Meteorol. Soc. 79, 61–78.

van der Maaten, E., van der Maaten-Theunissen, M., Buras, A., Scharnweber, T., Simard, S., Kaiser, K., Lorenz, S., Wilmking, M., 2015. Can We Use Tree Rings of Black Alder to Reconstruct Lake Levels? A Case Study for the Mecklenburg Lake District, Northeastern Germany. PLoS ONE 10 (8), e0137054. https://doi.org/10.1371/journal.pone.0137054.

van der Maaten-Theunissen, M., van der Maaten, E., Bouriaud, O., 2015. pointRes: an R package to analyze pointer years and components of resilience. Dendrochronologia 35, 34–38. https://doi.org/10.1016/j.dendro.2015.05.006.

Vesipa, R., Camporeale, C., Ridolfi, L., 2017. Effect of river flow fluctuations on riparian vegetation dynamics: Processes and models. Adv. Water Resour. 110, 29–50. https://doi.org/10.1016/j.advwatres.2017.09.028.

Vicente-Serrano, S.M., Beguer'a, S., López-Moreno, J.I., 2010. A multiscalar drought index sensitive to global warming: the standardized precipitation evapotranspiration index. J. Clim. 23, 1696–1718.

Vicente-Serrano, S.M., Gouveia, C., Camarero, J.J., Beguería, S., Trigo, R., Lopez-Moreno, J.I., et al., 2013. Response of vegetation to drought time-scales across global land biomes. Proc. Natl. Acad. Sci. 110, 52–57.

Werf van der, G.W., Sass-Klaassen, U., Mohren, G.M.J., 2007. The impact of the 2003 summer drought on the intra-annual growth pattern of beech (*Fagus sylvatica* L.) and oak (*Quercus robur* L.) on a dry site in the Netherlands. Dendrochronologia 25 (2), 103–112. https://doi.org/10.1016/j.dendro.2007.03.004.

Wigley, T.M.L., Briffa, K.R., Jones, P.D., 1984. On the average value of correlated time series with application in dendroclimatology and hydrometeorology. J. Appl. Meteorol. Clim. 23, 201–221.

Wiles, G.C., Krawiec, A.C., D'Arrigo, R.D., 2009. A 265-year reconstruction of Lake Erie water levels based on North Pacific tree rings. Geophys. Res. Lett. 36 (5), L05705. https://doi.org/10.1029/2009GL037164.

Willms, C.R., Pearce, D.W., Rood, S.B., 2006. Growth of riparian cottonwoods: a developmental pattern and the influence of geomorphic context. Trees 20, 210–218.

Worbes, M., 1999. Annual growth rings, rainfall dependent growth and long–term growth patterns of tropical trees from the Forest Reserve Caparo in Venezuela. J. Ecol. 87, 391–403.

Xu, H., Zhang, Z.Q., Chen, J.Q., Xiao, J.F., Zhu, M.X., Kang, M.C., Cao, W.X., 2018. Regulations of cloudiness on energy partitioning and water use strategy in a riparian poplar plantation Agric. For. Meteorol. 262, 135–146.

You, X., Liu, J., 2018. Modeling the spatial and temporal dynamics of riparian vegetation induced by river flow fluctuation. Ecol. Evol. 8 (7), 3648–3659. https://doi.org/10.1002/ece3.3886.

Zang, C., Biondi, F., 2015. Treeclim: An R package for the numerical calibration of proxy-climate relationships. Ecography (Cop.). 38, 431–436.

Zhang, J., Schurr, U., Davies, W.J., 1987. Control of stomatal behaviour by abscisic acid which apparently originates in the roots. J Exp Bot 38 (192), 1174–1181.

Zohary, T., Ostrovsky, I., 2011. Ecological impacts of excessive water level fluctuations in stratified freshwater lakes. Inland Waters 1, 47–59.